

Optimization of Sliding Mode with MRAS Based Estimation for Speed Sensorless Control of DSIM Via GWO

Abstract. Doing research on DSIM control and increasing its effectiveness and durability, made us think about using a strong estimating system to evaluate the speed and the rotor flux. So we are conducting this research based on the sliding mode speed sensorless vector control. Therien, we present the Model Reference Adaptive System (MRAS) of double stator induction motor is presented. In order to achieve a robust system, SMC controllers are designed to replace the current regulators of traditional vector control system and PI regulator of sensorless speed system. After trying this technique, we found it difficult to find the parameters of the sliding mode, so we suggest the use one metaheuristic method to find the optimal parameters, which is the Grey wolf to ensure robust control without a sensorless. The results presented to Matlab showed a positive effect on the behavior of the system, as presented the Grey Wolf in finding the optimal parameters, which enabled us to obtain a more robust system.

Streszczenie. Badania nad sterowaniem DSIM oraz zwiększeniem jego skuteczności trwałości skłoniły nas do zastanowienia się nad zastosowaniem silnego systemu szacowania do oszacowania prędkości i strumienia wirnika. Wykonaliśmy to badanie w oparciu o bezczujnikowe sterowanie wektorowe prędkości w trybie ślizgowym w oparciu o Model Odniesienia Systemu Adaptacyjnego (MOSA) silnika indukcyjnego z podwójnym stojanem. Dla uzyskania solidnego systemu, sterowniki STP zostały zaprojektowane w celu zastąpienia regulatorów prądu tradycyjnego systemu sterowania wektorowego i regulatora PI bezczujnikowego systemu prędkości. Po wypróbowaniu tej techniki stwierdziliśmy, że trudno jest znaleźć parametry trybu ślizgowego, dlatego zasugerowaliśmy użycie jednej metody metaheurystycznej w celu znalezienia optymalnych parametrów, czyli wilka szarego, aby zapewnić solidną kontrolę bez czujnika. Przedstawione Matlabowi wyniki wykazały pozytywny wpływ na zachowanie systemu, co pozwoliło nam uzyskać solidniejszy system. (Optymalizacja trybu przesuwu z szacowaniem opartym na MRAS dla bezczujnikowego sterowania prędkością DSIM za pośrednictwem GW)

Keywords: Dual Star Induction Motor (DSIM), field oriented control (FOC), sliding mode controller (SMC),.

Słowa kluczowe: Silnik Indukcyjny z Podwójną Gwiazdą (SIPG), Sterowanie Polowe (SP), Sterownik Trybu Przesuwne (STP),.

1. Introduction

The double stator induction machine (DSIM) needs a double three-phase supply, which has many advantages [1, 2]. It minimize the torque pulsations and uses power electronics components which allow a higher commutation frequency compared to the simple machines, However the double stator Induction machines supplied by a source inverter generate harmonics which result in supplementary losses [1]. The double star induction machine is not a simple system, because of a number of complicated phenomena, which appear in its function, as saturation and skin effects [3].

The double star induction machine is based on the principle of double stators displaced by $\alpha=30^\circ$ and rotor at the same time. The stators are similar to the stator of a simple induction machine and fed with 3 phases alternating current and provide a rotating flux. Each star is composed by three identical windings with their axes spaced by $2\pi/3$ [4, 5].

The field oriented control decoupling between these variables, and the torque is made similar as the one of a direct current machine [6]. One may note that the field oriented control scheme is very sensitive to induction machine parameters variations [7]. However, many problems, in order to apply the sensors, are the mounting of the sensor and the additional costs, etc [8].

MRAS is one of the best techniques due to its simplicity, good performance and stability. MRAS consists of reference model, an adaptive model and an adaptation mechanism.

Sliding mode controller with speed estimator has been suggested to achieve robust DSIM performance.

The sliding mode controller provides fast dynamic response, stable control system and easy access to hardware and software. Although this control method causes some defects associated with the large torque chattering that appears in steady state. Chattering involves high frequency control switching and may lead to excitation

of unmodelled high frequency system dynamics.

Chattering also causes high heat losses in electronic systems and undue wear in mechanical systems [9]. In order to reduce the system chattering a sign function is used.

Unfortunately, it has been very difficult to tune the gains of the SMC regulators correctly because many industrial plants are often overwhelmed by issues such as top order, lags, and non-linearities. It is difficult to determine the optimum or near optimum SMC (K and eps) parameter with conventional tuning methods. For all these reasons, it is very desirable to increase the capabilities of the SMC controller by adding new features.

Several approaches have been documented in the literature to determine the parameters of SMC, first found by Ziegler Nichols (ZN) tuning. Neural network, the fuzzy approach, and the Particle Swarm Optimization Techniques (PSO), GWO, Genetic Algorithm are just a few among many works. Grey Wolf Optimization (GWO) is recently developed meta-heuristics algorithm inspired from the leadership hierarchy and hunting mechanism of gray wolves in nature [10]. GWO has been successfully applied for solving the engineering optimization problems [11,12].

The rest of this paper, we present the SMC controller with a reference adaptive system model (MRAS) and compare the results with the classical PI controller. To increase the efficiency of DSIM the authors focus on the GWO with SMC controller to form a novel optimal SMC controller appropriate for reaching best dynamic performance of DSIM.

The Grey Wolf Optimization is introduced to solve multi-objectives functions of DSIM and extracting robust system are alleviated in order to find the optimal parameters of Sliding mode controller.

The results presented to Matlab showed a positive effect on the behavior of DSIM.

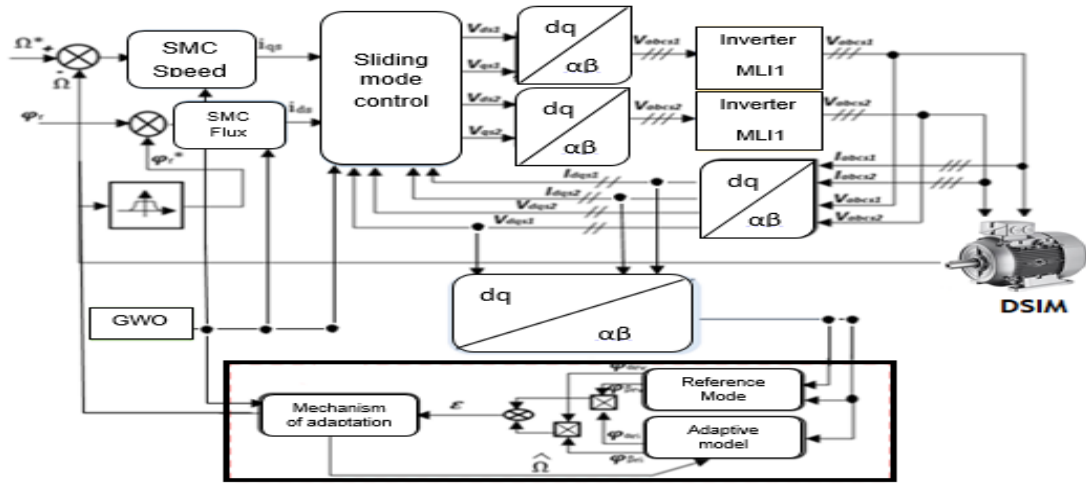


Fig.1.sliding mode sensorless vector control of DSIM.

2. Dynamic model of double star induction motor

A schematic of the stator and rotor windings for a machine dual three phase is given in Figure1. The six stator phases are divided into two wye-connected three phase sets labelled A_{s1}, B_{s1}, C_{s1} and A_{s2}, B_{s2}, C_{s2} whose magnetic axes are displaced by an arbitrary angle α . The windings of each three phase set are uniformly distributed and have axes that are displaced 120° apart. The three phase rotor windings A_r, B_r, C_r are also sinusoidally distributed and have axes that are displaced apart by 120° [13,14].

- The following assumptions are made:
- Motor windings are sinusoidally distributed;
 - The two stars have same parameters;
 - Flux path is linear.

The voltage equation is [15]:

$$(1) \begin{cases} [v_{abc,s1}] = R_s [i_{abc,s1}] + \frac{d}{dt} [\phi_{abc,s1}] \\ [v_{abc,s2}] = R_s [i_{abc,s2}] + \frac{d}{dt} [\phi_{abc,s2}] \\ [v_{abc,r}] = R_r [i_{abc,r}] + \frac{d}{dt} [\phi_{abc,r}] \end{cases}$$

$$(2) \begin{bmatrix} [\phi_{abc,s1}] \\ [\phi_{abc,s2}] \\ [\phi_{abc,r}] \end{bmatrix} = \begin{bmatrix} [L_{s1,s1}] & [L_{s1,s2}] & [L_{s1,r}] \\ [L_{s2,s1}] & [L_{s2,s2}] & [L_{s2,r}] \\ [L_{r,s1}] & [L_{r,s2}] & [L_{r,r}] \end{bmatrix} \begin{bmatrix} [I_{abc,s1}] \\ [I_{abc,s2}] \\ [I_{abc,r}] \end{bmatrix}$$

With

$$\begin{aligned} [v_{abc,s1}] &= [v_{as1} v_{bs1} v_{cs1}]^T; [v_{abc,s2}] = [v_{as2} v_{bs2} v_{cs2}]^T; \\ [I_{abc,s1}] &= [I_{as1} I_{bs1} I_{cs1}]^T; [I_{abc,s2}] = [I_{as2} I_{bs2} I_{cs2}]^T; \\ [v_r] &= [v_{ar} v_{br} v_{cr}]^T; [I_r] = [I_{ar} I_{br} I_{cr}]^T; \\ [R_{s1}] &= [R_{s2}] = \text{Diag}[R_s]_{(3 \times 3)}; \\ [R_r] &= \text{Diag}[R_r]_{(3 \times 3)}; \end{aligned}$$

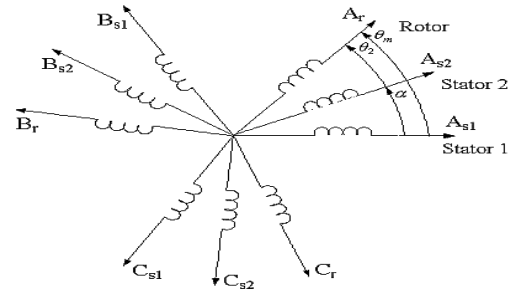


Fig.2. Windings of the DSIM.

The detail of the sub matrixes is given in the Appendix.

Where $R_{s1} = R_{s2}$; $L_{s1} = L_{s2}$ and L_{ms} are the stator resistance, leakage inductance and magnetizing inductance; R_r, L_r and L_{mr} the rotor resistance, leakage inductance and magnetizing inductance; M_{sr} Maximal mutual inductance between stator and rotor.

The Park model of DSIM is presented below in the references frame at the rotating field (d,q) [14,16,17]:

$$(3) \begin{cases} v_{ds1} = R_{s1} i_{ds1} + p\phi_{ds1} - \omega_s \phi_{qs1} \\ v_{qs1} = R_{s1} i_{qs1} + p\phi_{qs1} + \omega_s \phi_{ds1} \\ v_{ds2} = R_{s2} i_{ds2} + p\phi_{ds2} - \omega_s \phi_{qs2} \\ v_{qs2} = R_{s2} i_{qs2} + p\phi_{qs2} + \omega_s \phi_{ds2} \\ v_{dr} = R_r i_{dr} + p\phi_{dr} - (\omega_s - \omega_r) \phi_{qr} \\ v_{qr} = R_r i_{qr} + p\phi_{qr} + (\omega_s - \omega_r) \phi_{dr} \end{cases}$$

The expressions for stator and rotor flux are:

$$(4) \begin{cases} \phi_{ds1} = L_{s1} i_{ds1} + L_m (i_{ds1} + i_{ds2} + i_{dr}) \\ \phi_{qs1} = L_{s1} i_{qs1} + L_m (i_{qs1} + i_{qs2} + i_{qr}) \\ \phi_{ds2} = L_{s2} i_{ds2} + L_m (i_{ds1} + i_{ds2} + i_{dr}) \\ \phi_{qs2} = L_{s2} i_{qs2} + L_m (i_{qs1} + i_{qs2} + i_{qr}) \\ \phi_{dr} = L_r i_{dr} + L_m (i_{qs1} + i_{qs2} + i_{qr}) \\ \phi_{qr} = L_r i_{qr} + L_m (i_{qs1} + i_{qs2} + i_{qr}) \end{cases}$$

With $p = d/dt$; $3L_m/2 = L_{ms} = L_{mr} = L_{sr}$.

In the induction machines, rotor windings are short circuited hence, i.e. $v_{dr} = 0$ and $v_{qr} = 0$.

A. Mechanical Equation

The mechanical is given as follow [14,18]:

$$(5) \quad J \frac{d\Omega}{dt} = T_{em} - T_r - K_f \Omega$$

With

$$(6) \quad T_{em} = p \frac{L_m}{L_m + L_r} [\phi_{dr}(i_{qs1} + i_{qs2}) - \phi_{qr}(i_{ds1} + i_{ds2})]$$

3. Field oriented control of double star induction motor

The objective of space vector control is to assimilate the operating mode of the asynchronous machine at the one of a DC machine with separated excitation, by decoupling the torque and the flux control. With this new technique of control and microprocessor development we can obtain speed and torque control performances comparable at those of DC machine [18].

By applying field oriented control principle

($\phi_{dr} = \phi_r$ and $\phi_{qr} = 0$) to equations (3) ,(4) (5) and

(6), the field-oriented model of the motor is given by the following equation system:

$$(7) \quad \begin{cases} \frac{di_{ds1}}{dt} = \frac{1}{L_{s1}} \left[V_{ds1} - R_{s1}i_{ds1} - a_2(a_3(i_{ds1} + i_{ds2}) - a_4\phi_r) + \omega_s[(L_{s1} + a_1)i_{qs1} + a_1i_{qs2}] \right] \\ \frac{di_{qs1}}{dt} = \frac{1}{L_{s1}} \left[V_{qs1} - R_{s1}i_{qs1} - \omega_s[(L_{s1} + a_1)i_{ds1} + a_1i_{ds2} + a_2\phi_r] \right] \\ \frac{di_{ds2}}{dt} = \frac{1}{L_{s2}} \left[V_{ds2} - R_{s2}i_{ds2} - a_2(a_3(i_{ds1} + i_{ds2}) - a_4\phi_r) + \omega_s[(L_{s2} + a_1)i_{ds2} + a_1i_{ds1}] \right] \\ \frac{di_{qs2}}{dt} = \frac{1}{L_{s2}} \left[V_{qs2} - R_{s2}i_{qs2} - \omega_s[(L_{s2} + a_1)i_{ds2} + a_1i_{ds1}] \right] \\ \frac{d\phi_r}{dt} = a_3(i_{ds1} + i_{ds2}) - a_4\phi_r \\ T_{em} = p \frac{L_m}{L_m + L_r} \phi_r (i_{qs1} + i_{qs2}) \\ \frac{d\omega_r}{dt} = a_6 T_{em} - a_6 T_r - a_7 \omega_r \end{cases}$$

With :

$$\begin{aligned} a_1 &= \frac{L_m L_r}{L_m + L_r} ; a_2 = \frac{L_m}{L_m + L_r} \\ a_3 &= \frac{R_r L_m}{L_m + L_r} , a_4 = \frac{R_r}{L_m + L_r} \\ a_5 &= \frac{p L_m}{L_m + L_r} , a_6 = \frac{T_r}{J} , a_7 = \frac{K_f}{J} \end{aligned}$$

The expressions of the rotor currents may be given as:

$$(8) \quad i_{dr} = \frac{1}{L_r + L_s} [\phi_r - L_m(i_{ds1} + i_{ds2})]$$

$$(9) \quad i_{qr} = -\frac{L_m}{L_r + L_m} (i_{qs1} + i_{qs2})$$

$$(10) \quad \omega_{gl} = \frac{R_r}{L_m + L_r} (i_{qs1} + i_{qs2})$$

4. Adaptive system with reference model (MRAS)

Speed estimation based on MRAS is one of the best techniques due to its simplicity, good performance and stability [19]. In MRAS the reference model estimator is based on stator voltage model which does not contain the rotor speed parameter and adjustable model is based on current model which contains the rotor speed. The basic concept of MRAS is that the reference model and adaptive model independently estimates the required machine parameter using measured stator voltages and currents in the corresponding reference frame, in this work stationary reference frame is considered. The parameter estimated by the reference model and adaptive models are compared and the difference between them is the speed-tuning signal, which is tuned using an adaptation technique, and adjusts the adaptive model to reduce the error between them to zero. When the error between reference and adaptive model reduced to zero, the estimated speed is equal to the actual rotor speed of the drive. The adaptation mechanism should satisfy the Popov's criterion of hyper stability. Based on the speed-tuning signal MRAS can be classified in to three types, Rotor flux MRAS, Back emf MRAS and Reactive power MRAS and the mathematical equations for reference model and adaptive models are given in [20].

The basis of Rotor flux (RF) based MRAS is that rotor flux may be estimated either using the voltage model or the current model of an induction motor. The structure of reference model (RM) and adjustable model (AM) may be realized as follows:

4.1. Rotor Flux Based MRAS

a) Reference model

the reference rotor flux components obtained from the reference model are given by [21]:

$$(11) \quad \begin{cases} \frac{d\hat{\phi}_{r\alpha-v}}{dt} = \frac{L_m + L_r}{L_m} \left[\frac{V_{s\alpha1} - R_{s1}i_{s\alpha1} - \sigma(L_s + L_m) \frac{di_{s\alpha1}}{dt}}{L_m + L_r} - \frac{L_m L_r}{L_m + L_r} \frac{di_{s\alpha2}}{dt} \right] \\ \frac{d\hat{\phi}_{r\beta-v}}{dt} = \frac{L_m + L_r}{L_m} \left[\frac{V_{s\beta1} - R_{s1}i_{s\beta1} - \sigma(L_s + L_m) \frac{di_{s\beta1}}{dt}}{L_m + L_r} - \frac{L_m L_r}{L_m + L_r} \frac{di_{s\beta2}}{dt} \right] \end{cases}$$

b) Adaptive model

the adaptive model is described by the current model [24]:

$$(12) \quad \begin{cases} \frac{d\hat{\phi}_{r\alpha-i}}{dt} = \left[\frac{L}{T_r} (i_{s\alpha1} + i_{s\alpha2}) - \frac{1}{T_r} \hat{\phi}_{r\alpha-i} - \omega_r \hat{\phi}_{r\beta-i} \right] \\ \frac{d\hat{\phi}_{r\beta-i}}{dt} = \left[\frac{L}{T_r} (i_{s\beta1} + i_{s\beta2}) - \frac{1}{T_r} \hat{\phi}_{r\beta-i} + \omega_r \hat{\phi}_{r\alpha-i} \right] \end{cases}$$

c) Adaptation mechanism

The error between the reference model and the adjustable model is defined as follows:

$$(13) \quad \varepsilon = \hat{\phi}_{r\alpha-i} \hat{\phi}_{r\beta-v} - \hat{\phi}_{r\alpha-v} \hat{\phi}_{r\beta-i}$$

The adaptation law is classically given by a PI controller of the following expression [26, 20]:

$$(14) \quad \hat{\omega} = \varepsilon \left(k_p + \frac{k_i}{s} \right)$$

The speed resulting from (14) is in turn reinjected

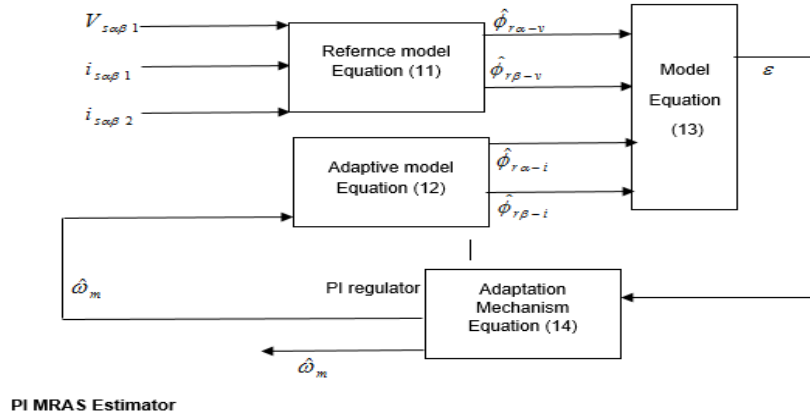


Fig.3. Block diagram of the classical MRAS technique applied to the DSIM.

In order to give a more robust system, given the unsatisfactory results given by Classic PI [21], So we introduced a more powerful regulator, which are based on a sliding mode technique.

5. Sliding mode control design

The basic principle of the sliding mode control consists in moving the state trajectory of the system toward a surface $S(x) = 0$ and maintaining it around this surface with the switching logic function U_n . The basic sliding mode control law is expressed as.

$$(15) \quad U_c = U_{eq} + U_n$$

This expression uses two terms, U_c and U_n , U_{eq} is determined off line with a model that represents the plant as accurately as possible. It is used when the system state is in the sliding mode. The term U_n : is a sign function defined as $U_n = k \text{sign}(S(x))$, where;

$$(16) \quad \text{sign}(S(x)) = \begin{cases} 1 & \text{if } |S(x)| < 0 \\ -1 & \text{if } |S(x)| > 0 \end{cases}$$

This will guarantee that the state is attracted to the switching surface by satisfying the Lyapunov stability:

$$(17) \quad S(x) \dot{S}(x) < 0$$

This strategy enforces the system trajectory to move toward and to stay on the sliding surface from any initial condition. Using a sign function often causes chattering in practice. One solution to reduce chattering is to introduce a boundary layer around the sliding surface [23],[24] [25]. This is expressed by:

into the adjustable model in such a way that the error converges. The speed resulting from (14) is in turn reinjected into the adjustable model in such a way that the error converges to zero.

From these results, it is obvious that for the reference model we will take the reference value of rotor flux in (11), and since (12) asks the information of the speed, it will be taken for the adjustable model this is shown in Figure 3

$$(18) \quad U_n = \begin{cases} k S(x) & \text{if } |S(x)| < \varepsilon \\ \varepsilon & \text{if } |S(x)| > \varepsilon \\ k \text{sgn}(S(x)) & \text{if } |S(x)| > \varepsilon \end{cases}$$

With k , a positive coefficient and ε , the thickness of the boundary layer. However, a small value of ε might produce a boundary layer so thin that it can excite high frequency dynamics [26].

6. Sliding mode control of double star induction motor Design of the switching surfaces

In this work six sliding surfaces are used and taken as follows since a first order model is used .

$$(19) \quad \begin{aligned} S(\omega_r) &= \omega_r^* - \omega_r \\ S(\phi_r) &= \phi_r^* - \phi_r \\ S(i_{ds1}) &= I_{ds}^* - i_{ds1} \\ S(i_{ds2}) &= I_{ds}^* - i_{ds2} \\ S(i_{qs1}) &= I_{qs}^* - i_{qs1} \\ S(i_{qs2}) &= I_{qs}^* - i_{qs2} \end{aligned}$$

With ω_r^* and ϕ_r^* are respectively the reference variables of the rotor speed and the flux. $S(\omega_r), S(\phi_r)$ are related to the outer loops, whereas $S(i_{ds1}), S(i_{ds2}), S(i_{qs1}), S(i_{qs2})$ are related to the inner loops. The i_{ds}^* and i_{qs}^* reference are determined by the outer loops ,and take respectively that values of the control variables i_{ds} and i_{qs} .

Development of the control laws

By using the equation systems (7) and (19), the regulators control laws are obtained as follows :

For the speed regulator

$$(20) \quad S(\omega_r) \cdot S'(\omega_r) < 0 \Rightarrow I_{qs}^* = i_{qs}^* + \lambda_1 \chi_1$$

$$\text{And } i_{qs}^* = i_{qseq} + i_{qsn}$$

$$\text{With } i_{qseq} = a_8 \frac{1}{\phi_r^*} [\omega^* + a_7 \omega_r + a_6 C_r]$$

$$a_8 = \frac{J(L_m + L_r)}{P^2 * L_m}$$

$$i_{qsn} = \begin{cases} \frac{K_{\omega r}}{\varepsilon_{\omega r}} \cdot S(\omega_r) & \text{if } |S(\omega_r)| < \varepsilon_{\omega r} \\ K_{\omega r} \cdot \text{Sgn}(S(\omega_r)) & \text{if } |S(\omega_r)| > \varepsilon_{\omega r} \end{cases}$$

For the flux regulator

$$(21) \quad S(\phi_r) \cdot S'(\phi_r) < 0 \Rightarrow I_{ds}^* = i_{ds}^* + \lambda_2 \chi_2$$

$$\text{And } i_{ds}^* = i_{dseq} + i_{dsn}$$

$$i_{dseq} = \frac{1}{a_3} [\phi^* + a_4 \phi_r]$$

$$i_{dsn} = \begin{cases} \frac{K_{\phi r}}{\varepsilon_{\phi r}} \cdot S(\phi_r) & \text{if } |S(\phi_r)| < \varepsilon_{\phi r} \\ K_{\phi r} \cdot \text{Sgn}(S(\phi_r)) & \text{if } |S(\phi_r)| > \varepsilon_{\phi r} \end{cases}$$

The regulators control laws, for the control variables i_{ds1} , i_{ds2} and i_{qs1} , i_{qs2} of the internal loops are given by :

For the control variable i_{ds1} et i_{ds2}

$$(22) \quad S(i_{ds1}) \cdot S'(i_{ds1}) < 0 \Rightarrow v_{ds1} = v_{ds1eq} + v_{ds1n}$$

With

$$v_{ds1eq} = L_{s1} i_{ds}^* + R_{s1} i_{ds1} - \omega_s [L_{s1} i_{qs1} + T_r \phi_r \omega_{gl}]$$

$$v_{ds1n} = \begin{cases} \frac{K_{d1}}{\varepsilon_{d1}} \cdot S(i_{ds1}) & \text{if } |S(i_{ds1})| < \varepsilon_{d1} \\ K_{d1} \cdot \text{Sgn}(S(i_{ds1})) & \text{if } |S(i_{ds1})| > \varepsilon_{d1} \end{cases}$$

$$(23) \quad S(i_{ds2}) \cdot S'(i_{ds2}) < 0 \Rightarrow v_{ds2} = v_{ds2eq} + v_{ds2n}$$

With

$$v_{ds2eq} = L_{s2} i_{ds}^* + R_{s2} i_{ds2} - \omega_s [L_{s2} i_{qs2} + T_r \phi_r \omega_{gl}]$$

$$v_{ds2n} = \begin{cases} \frac{K_{d2}}{\varepsilon_{d2}} \cdot S(i_{ds2}) & \text{if } |S(i_{ds2})| < \varepsilon_{d2} \\ K_{d2} \cdot \text{Sgn}(S(i_{ds2})) & \text{if } |S(i_{ds2})| > \varepsilon_{d2} \end{cases}$$

For the control variable i_{qs1} et i_{qs2}

$$(24) \quad S(i_{qs1}) \cdot S'(i_{qs1}) < 0 \Rightarrow v_{qs1} = v_{qs1eq} + v_{qs1n}$$

$$\text{With } v_{qs1eq} = L_{s1} i_{qs}^* + R_{s1} i_{qs1} + \omega_s [L_{s1} i_{ds1} + \phi_r]$$

$$v_{qs1n} = \begin{cases} \frac{K_{q1}}{\varepsilon_{q1}} \cdot S(i_{qs1}) & \text{if } |S(i_{qs1})| < \varepsilon_{q1} \\ K_{q1} \cdot \text{Sgn}(S(i_{qs1})) & \text{if } |S(i_{qs1})| > \varepsilon_{q1} \end{cases}$$

$$(25) \quad S(i_{qs2}) \cdot S'(i_{qs2}) < 0 \Rightarrow v_{qs2} = v_{qs2eq} + v_{qs2n}$$

$$\text{With } v_{qs2eq} = L_{s1} i_{qs}^* + R_{s2} i_{qs2} + \omega_s [L_{s2} i_{ds2} + \phi_r]$$

$$v_{qs2n} = \begin{cases} \frac{K_q}{\varepsilon_q} \cdot S(i_{qs}) & \text{if } |S(i_{qs})| < \varepsilon_q \\ K_q \cdot \text{Sgn}(S(i_{qs})) & \text{if } |S(i_{qs})| > \varepsilon_q \end{cases}$$

- For estimated speed sliding mode surface

The sliding surface of the estimated speed is:

$$(26) \quad s(\varepsilon) = \varepsilon + M \int \varepsilon \cdot dt$$

Where $M > 0$ and $\varepsilon = \hat{\phi}_{r\alpha-i} \hat{\phi}_{r\beta-v} - \hat{\phi}_{r\alpha-v} \hat{\phi}_{r\beta-i}$

The derivative of $S(\varepsilon)$ gives :

$$(27) \quad \dot{s}(\varepsilon) = \dot{\varepsilon} + M \varepsilon$$

Where :

$$(28) \quad \dot{\varepsilon} = \dot{\hat{\phi}}_{r\alpha-i} \hat{\phi}_{r\beta-v} + \hat{\phi}_{r\alpha-i} \dot{\hat{\phi}}_{r\beta-v} - \dot{\hat{\phi}}_{r\alpha-v} \hat{\phi}_{r\beta-i} - \hat{\phi}_{r\alpha-v} \dot{\hat{\phi}}_{r\beta-i}$$

the substituting of the adaptive model equation (12) into (28):

$$(29) \quad \begin{aligned} \dot{\varepsilon} = & \hat{\phi}_{r\alpha-i} \dot{\hat{\phi}}_{r\beta-v} - \dot{\hat{\phi}}_{r\alpha-v} \hat{\phi}_{r\beta-i} \\ & + \frac{L_m}{T_r} [(i_{s\alpha 1} + i_{s\alpha 2}) \hat{\phi}_{r\beta-v} - (i_{s\beta 1} + i_{s\beta 2}) \hat{\phi}_{r\alpha-v}] \\ & - \frac{1}{T_r} [\hat{\phi}_{r\alpha-i} \hat{\phi}_{r\beta-v} + \hat{\phi}_{r\alpha-v} \hat{\phi}_{r\beta-i}] \\ & - \hat{\omega}_m [\hat{\phi}_{r\beta-i} \hat{\phi}_{r\beta-v} + \hat{\phi}_{r\alpha-i} \hat{\phi}_{r\alpha-v}] \end{aligned}$$

By letting:

$$(30) \quad \begin{aligned} \chi_1 = & \hat{\phi}_{r\alpha-i} \dot{\hat{\phi}}_{r\beta-v} - \dot{\hat{\phi}}_{r\alpha-v} \hat{\phi}_{r\beta-i} \\ & + \frac{L_m}{T_r} [(i_{s\alpha 1} + i_{s\alpha 2}) \hat{\phi}_{r\beta-v} - (i_{s\beta 1} + i_{s\beta 2}) \hat{\phi}_{r\alpha-v}] \\ & - \frac{1}{T_r} [\hat{\phi}_{r\alpha-i} \hat{\phi}_{r\beta-v} + \hat{\phi}_{r\alpha-v} \hat{\phi}_{r\beta-i}] \end{aligned}$$

$$(31) \quad \chi_2 = \hat{\phi}_{r\beta-i} \dot{\hat{\phi}}_{r\beta-v} + \hat{\phi}_{r\alpha-i} \dot{\hat{\phi}}_{r\alpha-v}$$

Equation (27) and (29) can be written as :

$$(32) \quad \dot{\varepsilon} = \chi_1 - \hat{\omega}_m \chi_2$$

And

$$(33) \quad \dot{S}(\varepsilon) = \chi_1 - \hat{\omega}_m \chi_2 + M \varepsilon$$

By replacing with $\hat{\omega}_m$ equivalent and attractive control

$\hat{\omega}_m = \hat{\omega}_{m-eq} + \hat{\omega}_{m-n}$ in equation (33), we find:

$$(34) \quad \dot{S}(\varepsilon) = \chi_1 - \hat{\omega}_{m-eq} \chi_2 - \hat{\omega}_{m-n} \chi_2 + M\varepsilon$$

During sliding mode and in the established regime, we have $S(\varepsilon) = 0$ and therefore $\dot{S}(\varepsilon) = 0$ and $\hat{\omega}_{m-n} = 0$ hence :

$$(35) \quad \hat{\omega}_{m-eq} = \frac{\chi_1 + M\varepsilon}{\chi_2}$$

During the convergence mode, the Lyapunov condition (17) must be checked. By replacing (35) into (34) we obtain:

$$(36) \quad \dot{S}(\varepsilon) = \hat{\omega}_{m-n} \chi_2$$

We take for the attractive control :

$$(37) \quad \hat{\omega}_{m-n} = k_\varepsilon \frac{S(\varepsilon)}{|S(\varepsilon)| + \xi_\varepsilon}$$

The block diagram of the sliding mode MRAS estimator is shown in Fig.4:

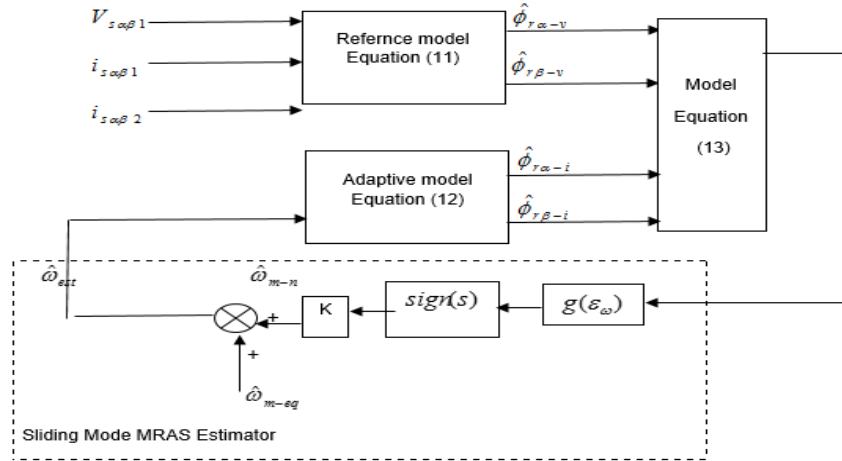


Fig.4. Block diagram of the sliding mode MRAS technique applied to the DSIM.

To test the sliding system, give good results, and eliminate the problem of finding its parameters, we have added one metaheuristics methods GWO. And we will explain it in the results obtained.

7. Controller optimization

For optimization of K and ξ in sign function SMC MRAS via GWO Matlab/Simulink model based on fig.1.

7.1. GWO Optimization of SMC Controller

The GWO algorithm [10] is a new meta-heuristic algorithm introduced in 2014 by Mirjalili et al. The GWO algorithm mimics the hierarchy of leadership and the mechanism of hunting gray wolves in the wild. The method simulates social hierarchy and hunting behavior in the society of gray wolves. Four types of simulations are applied in the gray wolf hierarchy:

Alpha (α), Beta (β), Delta (δ), and Omega (ω), as shown in Figure 5.

The Alpha Wolf (α) whose leaders of the whole group are primarily responsible for making decisions regarding hunting, sleeping, waking time, etc. Wolf Beta (β) which the subordinate of Wolf Alpha (α) is second in the hierarchy. The beta wolf (β) is known as the assistant of the Alfa (α) wolf in the decision of hunting and other activities. The lowest ranking the gray wolf is an omega wolf (ω) which follows the alphas (α), and Bêtas (β), but dominates the omega wolves (ω). If a wolf is not an Alpha (α), Beta (β) or Omega (ω), it is called a Delta wolf (δ). The search in GWO begins with the population of wolves (solutions) which are randomly generated. These wolves estimate the location of prey (optimal) by an iterative procedure during the hunting process (optimization). Alpha (α) is the most suitable solution followed by Beta (β) and Delta (δ) as the second and third best solution. The other solutions are the least important and considered as Omega (ω) [10]. The hunting behavior is mainly divided into three stages [10]:

a) Follow, hunt and approach the prey.

- Surround and harass the prey until it stops de bouger.
- Attack the prey.

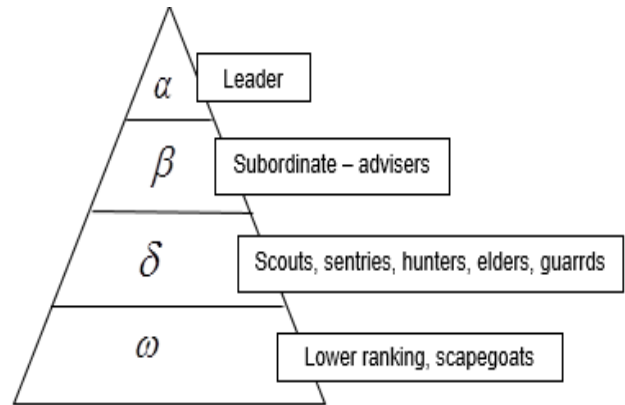


Fig.5. the grey wolf heirarchy.

The following equations modeling the circling behavior

$$(38) \quad \vec{D} = \left| \vec{C} \vec{X}_p(t) - \vec{X}(t) \right|$$

$$(39) \quad \vec{X}(t+1) = \vec{X}_p(t) - \vec{A} \vec{D}$$

where t is the current iteration, A and C are coefficient vectors, X_p represents the position of the victim. X indicates

The position vectors of the grey wolf. The vector A and C are calculated as follows:

$$(40) \quad \vec{A} = 2a\vec{r}_1 - \vec{a}$$

$$(41) \quad \vec{C} = 2\vec{r}_2$$

$$(42) \quad \vec{D}_\alpha = \left| \vec{C}_1 \vec{X}_\alpha - \vec{X} \right|, \vec{D}_\beta = \left| \vec{C}_2 \vec{X}_\beta - \vec{X} \right|, \vec{D}_\delta = \left| \vec{C}_3 \vec{X}_\delta - \vec{X} \right|$$

$$(43) \quad \bar{X}_1 = \bar{X}_\alpha - \bar{A}_1(\bar{D}_\alpha), \bar{X}_2 = \bar{X}_\beta - \bar{A}_2(\bar{D}_\beta), \bar{X}_3 = \bar{X}_\delta - \bar{A}_3(\bar{D}_\delta),$$

$$(44) \quad \bar{X}(t+1) = \frac{\bar{X}_1 + \bar{X}_2 + \bar{X}_3}{3}$$

The GWO pseudo-code is shown in Figure 6. In the GWO algorithm, the mathematical models of the social hierarchy are made up of; tracking, encircling and attacking prey are described in Mirjalili et al. [23]. The parameters of the GWO algorithm are given in Table 1.

```

Initialize the grey wolf population =(i=1,2,...,n)
Initialize Alpha, Beta , and Delta
Calculate the fitness of each search agent
Xα = the best search agent
Xβ = the second best search agent
Xγ = the third best search agent
While (t < Max number of iteration )
    for each search agent
        update the position of the current search agent by equation (43)
    end for
    Update Alpha, Beta , and Delta
    Calculate the fitness of all search agents
    Update Xα , Xβ , Xγ
    t = t + 1
end while
return Xα

```

Fig6. Pseudo code of the GWO Algorithm.

Table.1: Grey Wolf Optimizer Parameters

Maximum Iteration	60
Number of search Agent	15

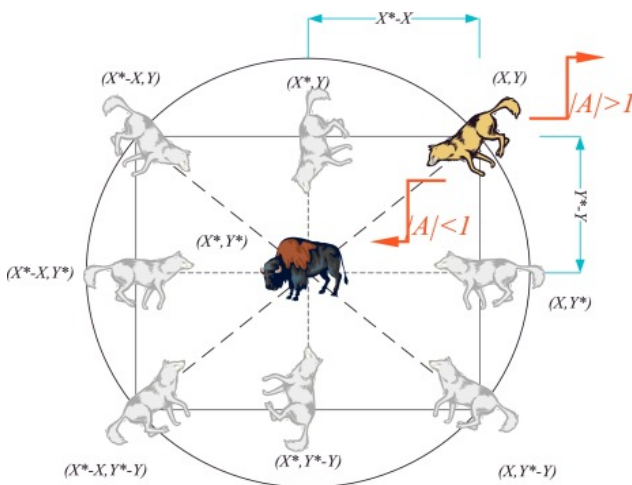


Fig.7. positioning mechanism of the search agent and the effect of what presents it [10].

8. Simulation results

The parameters of the simulated system are presented in -the appendix A. Simulation tests were carried out to compare the system of DSMI with PI, SMC, and SMC_GWO. Using an indirect vector control dual star induction motor. The tests were performed in both open loop and sensorless modes of operation. Selected simulation results from these tests are shown in the following sections.

Table.2. the parameters of pi, SMC and the best solution obtained by GWO.

PI Controller	$K_{p_{wr}}$	$k_{i_{wr}}$	K_p	K_i	$K_{p_{w-est}}$	$K_{i_{w-est}}$
	0.78	3.13	110	1420	0.56	1420
SMC Controller Gains	K_{wr}	ξ_{wr}	K_{ϕ_r}	ξ_{ϕ_r}	K_{d1}	ξ_{d1}
	100	0.4	120	0.01	1500	0.12
	K_{q1}	ξ_{q1}	K_{d2}	ξ_{d2}	K_{q2}	ξ_{q2}
	1000	0.18	1500	0.12	1000	0.18
SMC-GWO	K_{wr}	ξ_{wr}	K_{ϕ_r}	ξ_{ϕ_r}	K_{d1}	ξ_{d1}
	250.84	0.62	271.9	0.14	110.57	0.95
	K_{q1}	ξ_{q1}	K_{d2}	ξ_{d2}	K_{q2}	ξ_{q2}
	2706.2	0.32	4372	0.47	4895.4	0.51

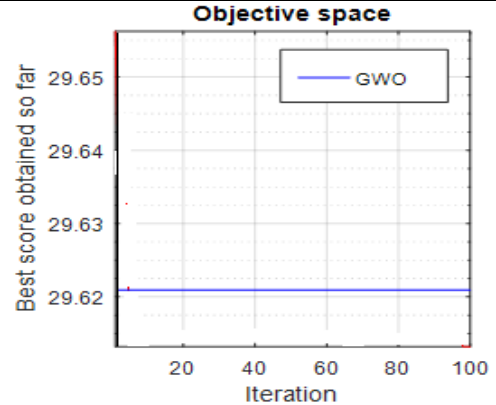


Fig8. The best solution of GWO.

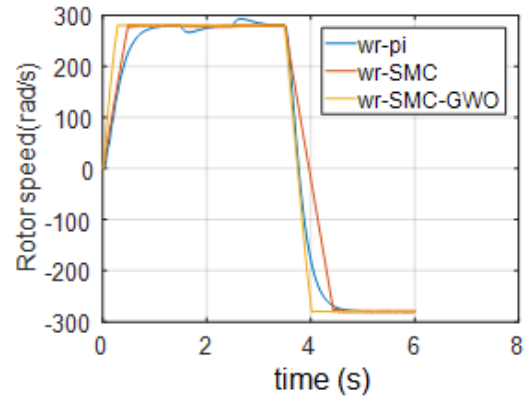


Fig9. Representation of estimated speed of DSIM

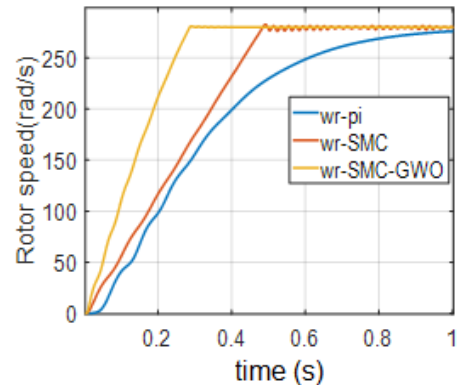


Fig10. Zoom of the first positive part.

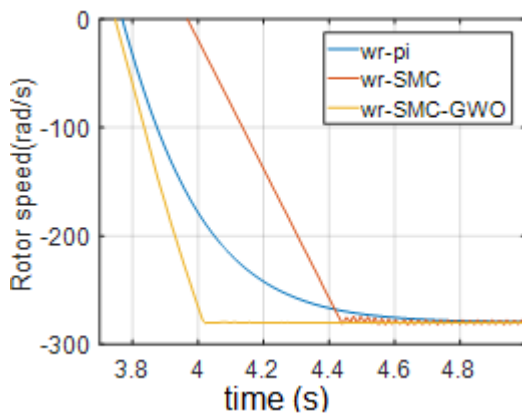


Fig11. Zoom of the second negative part.

The fig.8 shows the best fitness value of GWO versus iteration. The fig.9 presents the system's responses of the three proposed controllers.

The both SMC and SMC-GWO controllers are robust than PI which is affected by the change of the load. According to the figs 10-11 which show the zoom of the system's responses in the intervals [0 - 1] and [3.8 - 4.8] The controllers SMC-GWO is the faster and more robust.

9. Conclusion

In this research, the motor speed is estimated based on the flux rotor model reference adaptive method. Due to the large number of high-order harmonics and noise in the voltage model and the existence of the speed fluctuation problem in the traditional vector control system, the speed estimation accuracy and system dynamic performance are seriously affected. By the introduction of PI controllers, and according to Lyapunov's stability theorem, SMC controllers are designed to replace the current regulators of traditional vector control system and PI regulator of sensorless speed system.

In order to obtain the optimal value of the speed estimation, we did optimizing the SMC controllers using GWO. The simulation results show that noise of system and speed fluctuations are eliminated, and speed estimation accuracy and dynamic performance are obviously improved.

10. List of abbreviations

DSIM: Dual Star Induction Motor.
 PI: Proportional Integral controller.
 SMC: Sliding Mode Controller.
 MRAS: Adaptive System with Reference Model.
 GWO: Grey Wolf Optimizer.
 SMC_GWO: Sliding Mode Controller with Grey Wolf Optimizer.

11. Nomenclature

s: Index Stator.
 r: Index Rotor.
 Vds1, Vqs1, Vds2, Vqs2: Stator voltages d-q axis components.
 ids1, iqs1, ids2, iqs2: Stator currents d-q axis components.
 Rs1, Rs2: Stators resistances.
 φdr, φqr: Rotor flux d-q axis components.
 Rr, Rm: Rotor resistance, nominal resistance
 Ls1, Ls2: Stators inductances.
 Lr: Rotor Inductance.
 Lm: Mutual inductance.
 Ws: Speed of the synchronous reference frame.
 W: Rotor electrical angular speed.

Wgl: Slip speed.
 J: Moment of inertia.
 P: Number of pole pairs.
 Ω: Mechanical speed.
 Tem or Ce: Electromagnetic torque.
 TI or Cr: Load torque.
 fc: Friction coefficient.

12. Appendix:

Table.3. Nominal parameters of the DSIM used:

Rated power	4.5 kW
Rated voltage	220 V
Rated current	6.5 A
Rated speed	2840 rpm
Rated frequency	50 Hz
Rotor resistance Rr	2.12 Ω
Stator inductance Ls1= Ls2	0.011 H
Stator resistance Rs1= Rs2	3.72 Ω
Rotor inductance Lr	0.274 H
Magnetizing Inductance	0.3672 H
Number of pairs of poles 'P'	2
Rotor inertia J	0.0625 Kg.m2
Friction Coefficient fc	0.08m.s/rd

13. Acknowledgment

This work was financially supported by Intelligent Control and Electrical Power System Laboratory, University of Sidi Bel-Abbes, Algeria, the authors wish to thank the head of the laboratory.

Authors: Azeddine Beghdadi, He is a PhD in the Department of Electrical Engineering, He is a member in Intelligent Control and Electrical Power System Laboratory, University of Djillali Liabas, Sidi Bel-Abbes, Algeria E-mail: azeddine_beghdadi@yahoo.fr. Abderrahim BENTAALLAH, professor of Electrical Engineering, He is a member in Intelligent Control and Electrical Power System Laboratory (ISAPCE) at the University of Djillali Liabas, Sidi Bel-Abbes, Algeria Email: bentallah65@yahoo.fr. Abdellah ABDEN, He is a PhD in the Department of Electrical Engineering, He is a member in Smart Grids & Renewable Energies Laboratory (SRGE) at the University of Tahri Mohammed Bechar, BP 417 Route de Kenadsa, 08000 Bechar, Algeria, E-mail: abdenabd08@gmail.com.

REFERENCES

- [1] D. Hadiouche, H. Razik and A. Rezzoug, "Study and simulation of space vector PWM control of double-Star Induction Motors", 2000 *IEEE-CIEP*, Acapulco, Mexico, (2000), pp. 42-47.
- [2] G. K. Singh, K. Nam and S. K. Lim, "A simple indirect field oriented control scheme for multiphase induction machine", *IEEE Trans. Ind. Elec.*, vol. 52, no. 4, (2005) August, pp. 1177-1184.
- [3] D. Hadiouche, H. Razik and A. Rezzoug, "Modelling of a double-star induction motor with an arbitrary shift angle between its three phase windings", *EPE-PEMC 2000*, (2000), Kosice.
- [4] D. Casdei, G. Serra and A. Tani, "The use of converters in direct control of induction machines", *IEEE Trans*, on Industrial Electronics, vol. 48, no. 6, (2001).
- [5] T. S Radwan, "Perfect speed tracking of direct torque controlled induction motor drive using Fuzzy logic", *IEEE Trans Ind, Appl*, (2005), pp. 38-43.
- [6] T. Laamayad, F. Naceri, R. Abdessemed, S. Belkacem, "A Fuzzy Adaptive Control for Double Stator Induction Motor Drives," *The International conference on Electronics and Oil*, From Theory to Applications, Ouargla, Algeria, March 05-06, 2013.
- [7] G.R. Arab Markadeh, J. Soltani, N.R. Abjadi, M. Hajian, "Sensorless Control of a Six-Phase Induction Motors Drive Using FOC in Stator Flux Reference Frame," *International Journal of Mechanical, Aerospace, Industrial, Mechatronic and Manufacturing Engineering*, Vol.3, No.10, 2009.
- [8] M. A. Fnaiech, F. Betin, G. A. Capolino, "MRAS applied to sensorless control of a six phase induction machine," *IEEE*

- International Conference on Industrial Technology*, Vina del Mar, Chile, 14-17 March 2010.
- [9] A. Meroufel, A. Massoum, and P. Wira "A Fuzzy Sliding Mode Controller for a Vector Controlled Induction Motor", *Industrial Electronics*, 2008. ISIE 2008. *IEEE International Symposium on Publication*, pp. 1873-1878(2008),
- [10] S. Mirjalili, S.M. Mirjalili, and A. Lewis, "Grey wolf optimizer", *Advances in Engineering Software*, Vol.69, pp.46–61, 2014.
- [11] S. Gholizadeh, "Optimal design of double layer grids considering nonlinear behaviour by sequential grey wolf algorithm", *Journal of Optimization in Civil Engineering*, Vol. 5, No. 4, pp.511523, 2015.
- [12] A. El-Fergany, and H. M. Hasanien, "Single and multi-objective optimal power flow using grey wolf optimizer and differential evolution algorithms", *Electric Power Components and Systems*, Vol. 43.
- [13] D. Hadiouche, H. Razik and A. Rezzoug, "On the modeling and design of dual-stator windings to minimize circulating harmonic currents for VSI fed AC machines," *IEEE Trans. Ind. Appl.*, vol. 40, no. 2, pp. 506–515, March/April 2004.
- [14] G. K. Singh, K. Nam and S. K. Lim, "A simple indirect field-oriented control scheme for multiphase induction machine," *IEEE Trans. Ind. Elect.*, vol. 52, no. 4, pp. 1177–1184, August 2005.
- [15] M. Merabtene et E. R. Dehault, "Modélisation en vue de la commande de l'ensemble convertisseur-machine multi-phases fonctionnant en régime dégradé," Sixième conférence des jeunes chercheurs en génie électrique, *JCGE'3, Saint-Nazaire*, pp. 193–198, 5 et 6 Juin 2003.
- [16] D. Beriber, E. M. Berkouk, A. Talha and M. O. Mahmoudi, "Study and control two two-level PWM rectifiers-clamping bridge-two three-level NPC VSI cascade. Application to double stator induction machine," *35th Annual IEEE Electronics Specialists Conference*, pp. 3894–3899, Aachen, Germany, 2004.
- [17] V. Pant, G. K. Singh and S. N. Singh, "Modeling of a multi-phase induction machine under fault condition," *IEEE International Conference on Power Electronics and Drive Systems*, PEDS'99, pp. 92– 97, July 1999, Hong Kong.
- [18] Y. Fu, "Commande découplées et adaptatives des machines asynchrones triphasées," Thèse de doctorat, Université Montpellier II, 1991.
- [19] Y. Fu, "Commande découplées et adaptatives des machines asynchrones triphasées," Thèse de doctorat, Université Montpellier II, 1991.
- [20] Mini R, Shabana Backer P, B. Hariram Satheesh, Dinesh M. N "Low Speed Estimation of Sensorless DTC Induction Motor Drive Using MRAS with Neuro Fuzzy Adaptive Controller" *International Journal of Electrical and Computer Engineering (IJECE)*, ISSN: 2088-8708, Vol. 8, No. 5, pp. 2691~2702, October 2018.
- [21] Rabah Araria, Karim Negadi, Mohamed Boudiaf, Fabrizio Marignetti, Nonlinear control of DC-DC converters for battery power management in electric vehicle application, *Przeegląd Elektrotechniczny*, ISSN 0033-2097, R. 96 NR 3/2020.
- [22] Puli, A. Venkadesan (2014), "Comparison of Rotor Flux and EMF Based MRAS for Rotor Speed Estimation in Sensorless Direct Vector Controlled Induction Motor Drives", *IJRIT International Journal of Research in Information Technology*, Vol. 2, Issue 4, pp. 130-138.
- [23] E. Merabet, R. Abdessemed, H. Amimeur and F. Hamoudi, "Field oriented control of a dual star induction machine using fuzzy regulators," in *4th Int. Conf. Computer Integrated Manufacturing*, CIP'07, Univ. Setif, Algeria, Nov. 03–04, 2007.
- [24] Araria, R., Berkani, A., Negadi, K., Marignetti, F., Boudiaf, M. (2020). Performance analysis of DC-DC converter and DTC based fuzzy logic control for power management in electric vehicle application. *Journal Européen des Systèmes Automatisés*, Vol.53, No.1, pp.19. <https://doi.org/10.18280/jesa.530101>.
- [25] R. Bojoi, A. Tenconi, G. Griva and F. Profumo, "Vector control of dual three- phase induction-motor drives two current sensors," *IEEE Trans. Ind. Appl.*, vol. 42, no. 5, pp. 1284–1292, Sep./Oct. 2006.
- [26] R. Bojoi, M. Lazzari, F. Profumo and A. Tenconi, "Digital FieldOriented Control for Dual Three-Phase Induction Motor Drives", *IEEE Trans. On INDUSTRY Appl.*, Vol. 39, No. 3, (May/June)2003, pp.752-760.